Composites Research

Vol. 35, No. 3, 216-221 (2022)
DOI: http://dx.doi.org/10.7234/composres.2022.35.3.216
ISSN 2288-2103(Print), ISSN 2288-2111(Online)

Paper

Performance Study of Composite Air Filters Using Heterogeneous Fibers

Ji Soo Lee*,, Yuree Oh*, Heejin Kim*,**, Hyun-Seol Park***, Sam S. Yoon**†, Min Wook Lee*†**

ABSTRACT: Recently, the worldwide demand for disposable masks has increased due to COVID-19 infections and severe air pollution. Personal masks should reduce breathe resistance while maintaining filtering performance. In this study, a solution blowing process is used to produce composite nanofiber filters to co-spin two polymers at once. The manufacture process of the various fiber diameter filter was designed, and the filtration performance and differential pressure of the prepared filter was investigated. Poly vinylidene fluoride-hexafluoropropylene (PVDF-HFP) and Polylactic acid (PLA) fibers were chosen to be entangled together in a layer with a diameter of 1.05 μm and 0.33 μm. Composite nanofilters showed up to 87% filtration efficiency and 32 Pa differential pressure.

Key Words: Air filter, Composite, Heterogeneous fibers, Solution blow spinning

1. INTRODUCTION

The coronavirus disease (COVID-19) pandemic and severe air pollution, such as fine dust and yellow dust, have increased demand for disposable masks since the end of 2019. Using medical masks like N95 efficiently protects against infectious droplets and air pollution [1-3]. As a result, wearing a disposable mask for an extended period is essential to successfully prevent the spread of viruses or inhalation of particulate matter (PM). However, if a disposable mask is used for an extended period, it can cause breathing difficulties depending on the wearer's health condition [4]. Therefore, public attention is centered on how comfortable it is to wear and how easy it is to breathe. Microdiameter fibers produced by meltblowing PP (Polypropylene) or PET (Polyethylene Terephthalate) polymers are being used in disposable masks. Since large-diameter fibers have relatively large holes, the filter thickness is raised to achieve infection-prevention filtration performance, or several filters are employed [5,6]. A disadvantage exists in the case of a disposable mask with a nanofiber filter: the high differential pressure caused by small pore diameters disturbs the user's breathing. Furthermore, when the pores are small, the differential pressure rises rapidly because fine dust gathered in a mask clog the pores between the fibers when worn for an extended period. These issues contribute to a disposable mask's service life being cut short. Therefore, recent studies [7-9] have proposed a hybrid structure mixing large and small fibers or layering to solve each problem. This suggests that it may be useful in lowering pressure difference while retaining the filtering performance of a filter.

Roh *et al.* investigated the role of intra and interlayer space of filter media on the pressure drop development with continued particle loading. The intermingled structure of microfiber and nanofiber has higher porosity and improved quality factor (QF) than nanofiber [10]. ZheWang investigated multilayered filters with varying fiber diameter and fabricated a filter with high filtration performance and low pressure difference [7]. Yang *et al.* conducted an experiment to lower differential pressure by employing a fiber bead and securing a gap layer between fibers [9]. Shichao Zhang developed single-layer filters with varied fiber diameters using electrospinning [11]. Solution blow spinning (SBS) is a method used to produce fibers with nano-to-micro diameters. Concentric nozzles are used in SBS, with an inner nozzle extruding a polymer solution and an

Received 31 May 2022, received in revised form 20 June 2022, accepted 21 June 2022

*Institute of Advanced Composite Materials, Korea Institute of Science and Technology, Jeonbuk 55324, Korea
**School of Mechanical Engineering, Korea University, Seoul 02841, Korea
***Climate Change Technology Research Division, Korea Institute of Energy Research, Daejeon 34129, Korea
†Corresponding authors (E-mail: skyoon@korea.ac.kr, mwlee0713@kist.re.kr)

outer nozzle discharging high pressure gases (air, nitrogen, argon, etc.). The polymer solution forms droplets by being forced inflowing at a constant feed rate through an internal nozzle. High-pressure compressed gases passing through the external nozzle deform the polymer solution into a cone shape. When the surface tension of the solution is overcome, a solution jet is ejected and accelerated toward the target to be collected. During an ejection, the solvent is rapidly evaporated and polymer fibers are finally collected on a collector [12].

The SBS method has advantages of high yield, short preparation time, and high practicality. Because the SBS method is not limited by static electricity or the solution dielectric constant, it is suitable for voltage insensitive polymers, and the mass production of nanofibers and large-scale industrial production is possible. Accordingly, the SBS process has been receiving attention gradually recently as a new spinning technology. The SBS method has been widely used in various fields such as biopharmaceutical [13-16], energy materials [17-20], sensors [21,22], and filters [23-25]. The SBS process is used in this study to produce single-layer composite nanofiber filters with varied fiber diameters in a short period. The surface potential of the filter manufactured in the experiment was measured, and the spinning shape was compared to the performance efficiency of the filter.

2. EXPERIMENT

2.1 Materials

For this study, Polylactic acid (PLA) was purchased from Rainbox Filament by Hanil Industrial Co., Korea. Poly vinylidene fluoride-hexafluoropropylene (PVDF-HFP; Mw = 400 kDa) was purchased from Sigma-Aldrich, and acetone was purchased from SK chemical Co., Ltd, Korea.

2.2 Preparation of Solution Blown Filter Media

Each 12 wt% solution of PLA and PVDF-HFP was prepared in acetone at 35°C on a hot plate with magnetic stirring for 6 h. Two-stream solution blowing was performed for SBS by simultaneously solution blowing of PVDF-HFP solution and PLA solution from two perpendicular capillaries, as shown in Fig. 1. The polymer solution jet was released using an 18-gauge needle at a pumping rate of 30 mL/h. For single SBS, PVDF-HFP and PLA, air was released at a pressure of 0.4 MPa for 4 min. In the case of dual SBS, PVDF-HFP/PLA, air was released at a pressure of 0.4 MPa for 2 min. A vacuum was coupled to the bottom of the poly-propylene mesh to collect the blown fibers. The distance between vacuum-connected collection mesh and nozzles was 30 cm. The entire spinning process was conducted at 20 °C and the relative humidity of 30%.

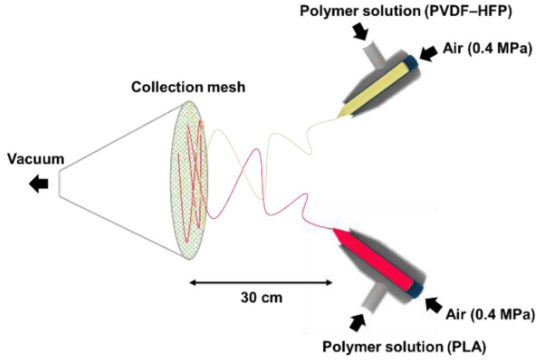

Fig. 1. Schematic of SBS simultaneous spinning

2.3 Characterization

Scanning electron microscopy (NovaNanoSEM450, FEI, USA) at a voltage of 20 kV was used to examine the morphology of the fibers and filtered PM. The as-spun fibers' pore size distribution was evaluated using a capillary flow porometer (CFP-1500Ae, Porous Materials Inc., USA) at 5 psi. Individual fiber diameters were measured from at least 100 points and averaged. Additionally, the surface potential of each sample was measured over time, as this affects the filter performance.

2.4 Filter test of Solution Blown Filter Media

All samples are exposed to ambient air for 24 h before the filter test. The PVDF-HFP and PLA sample were lightly clapped 20 times each other, and the non-rubbed cases were measured as well. The cases in which the sidewalls of the spun fibers were rubbed 20 times and the non-rubbed case was measured in the case of samples in which PVDF-HFP and PLA were simultaneously spun. All samples were cut in a 50 mm diameter.

The efficiency of as-spun fibers in filtering of aerosols was investigated by measuring the size distribution of aerosol at inlet and outlet of tested filters using a scanning mobility particle sizer (Model 3926, TSI, USA). Aerosol was generated by atomizing 1.0 wt% distilled water solution of potassium chloride (KCl). The distribution of particle sizes is presented in

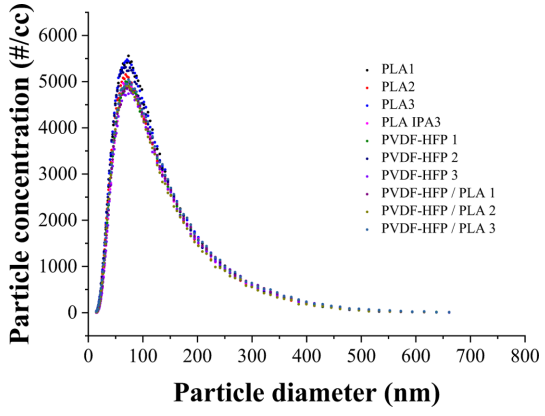

Fig. 2. Size distribution of KCl particles used in aerosol filtration test

Fig. 2. The size distribution of the KCl particles at the inlet was almost kept same in all the tests. The surface area of the respirator was approximately 25 cm^2, and the face velocity at 4.0 LPM corresponds to approximately 5.3 cm/s. The inlet/outlet concentration for the filtration efficiency was measured in the order of "IN-OUT-IN" at 3.7 LPM for each sample, and the inlet concentration was averaged as following Eq. (1).

$$\text{Filtration efficiency (\%)} = \frac{C_i - C_0}{C_i} \times 100 \quad (1)$$

3. RESULTS AND DISCUSSIONS

3.1 Morphology of Filter Media

The images of the as-spun fibers are summarized in Fig. 3. Fibers were prepared with 12 wt% PLA and PVDF-HFP solution, spun at 0.4 MPa and 30 cm distance for 4 min in single spinning, and 30 mL/h of flow rate for 2 min in simultaneous spinning. The diameters of the spun fibers were measured at 100 points and averaged. The distribution of fiber diameters is summarized as a histogram in Fig. 3. The average diameters of the PLA, PVDF-HFP, and PVDF-HFP/PLA were 1.05 ± 0.42, 0.33 ± 0.12, and 0.60 ± 0.40 μm, respectively. Despite the same solution concentration, PLA had a thicker fiber diameter than PVDF-HFP, and in the case of simultaneous spinning, fibers of various diameters could be confirmed through the diameter distribution diagram to be mixed.

To ensure that the two polymer fibers were uniformly mixed in the simultaneous-spun PVDF-HFP/PLA fibers, an F (fluorine) element mapping was done using EDS. The results are shown in Fig. 4. The green in the image showed the F element present in the PVDF-HFP. The PVDF-HFP fibers could be confirmed to be entangled with the PLA fibers, and the space between the PLA fibers was occupied by PVDF-HFP fibers making it better filter performance.

A pore distribution was measured examine the average pore size and pore distribution of the two types of spun fibers. The pore sizes of each fiber were 12.57 ± 0.96, 3.1 ± 80.32, and 5.78 ± 0.89 μm for PLA, PVDF-HFP, and PVDF-HFP/PLA, respectively, and the pore size distribution is shown in Fig. 5a. By forming different diameters, the two types of polymer solutions influence pore sizes. When seen in the pore size distribution diagram, the PLA with a large fiber diameter case could be confirmed of distributing over a wide range, and larger pore size than cases in spun with the PVDF-HFP only and spun simultaneously with the PVDF-HFP and PLA. Furthermore, as shown in Fig. 5b, the diameter and pore sizes could be seen as having the same tendency. PVDF-HFP/PLA is in between PLA and PVDF-HFP. As seen in the previous SEM (Scanning Electron Microscope) images, this was because the PLA fiber with a large diameter made a large space

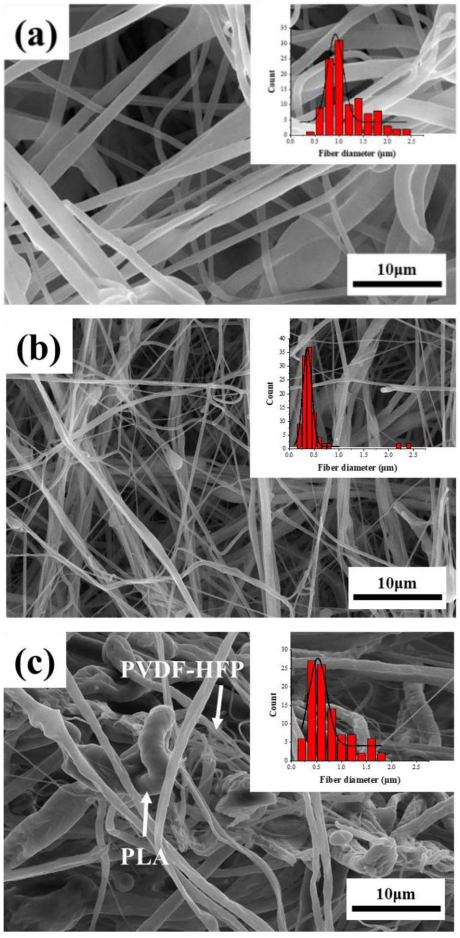

Fig. 3. SEM image and fiber diameter distribution of each as-spun fiber (a) PLA, (b) PVDF-HFP, (c) PVDF-HFP/PLA

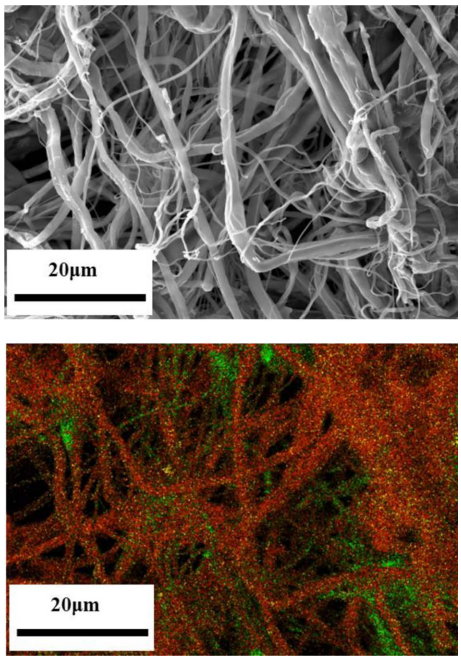

Fig. 4. Elemental mapping image of PVDF-HFP/PLA (X 1500, green: F)

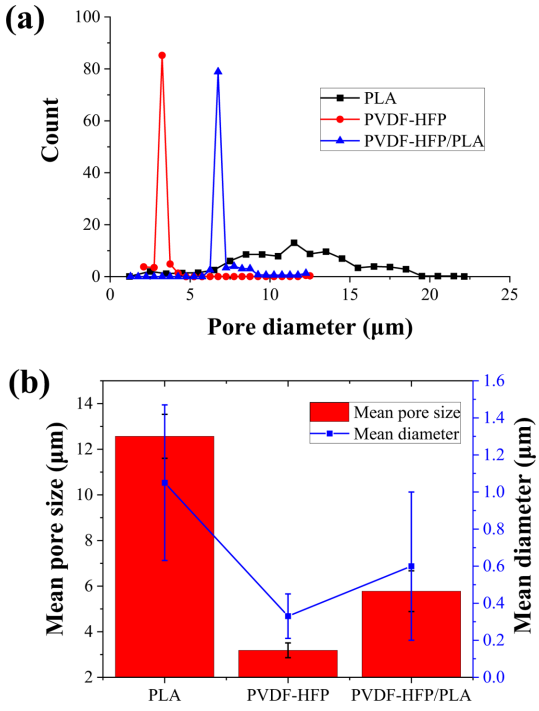

Fig. 5. (a) Pore size distribution of each spun fiber, (b) mean pore size and mean diameter

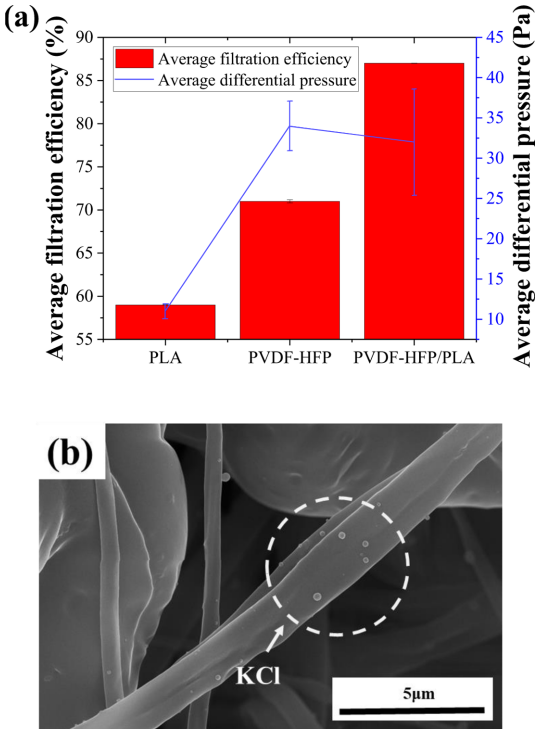

Fig. 6. (a) Filtration efficiency and differential pressure, (b) SEM image of PVDF-HFP/PLA after filter test (X8000)

between the fibers and thin PVDF-HFP fiber occupied the space. Thus, it was confirmed that the pores sizes could be controlled by SBS of the two fibers concurrently.

3.2 Filtration Performance and Differential Pressure

To confirm the filtration ability of heterogeneous fibers filters, a filtration test was performed. As shown in Fig. 6a, for the filtration performance, PLA, PVDF-HFP, and PLA/PVDF-HFP were measured by 59 ± 0.03%, 71 ± 0.18%, and 87 ± 0.02%, respectively, and the differential pressure by 11 ± 0.94, 34 ± 3.09, and 32 ± 6.60 Pa, respectively. When the results were compared, the PVDF-HFP sample showed higher efficiency and differential pressure than the other cases because the PVDF-HFP had smaller pores than the other cases. Compared to the other two cases, the PLA sample had the lowest filtration efficiency and differential pressure.

The previous findings showed that since the PLA had the largest fiber diameter and pores, particle matters could not be captured and escaped through the pores between the fibers.

In PLA/PVDF-HFP, the PLA fiber with a large diameter made a large space between the fibers and thin PVDF-HFP fiber occupied the space. that perhaps not only improve the capture ability of the particles but also prevent the penetration of air flow across the fibers. Thus, it is very important to optimize the structure, including through-pore size, and the combination form of fibers with different diameters, of composite membranes by dual SBS to gain high filtration efficiency with a relatively low pressure drop.

Table 1. Parameters of commercial respirators

Sample	Pressure drop (Pa)	Filtration efficiency (%)	Reference
N95 grade	87	99.5	[26]
KF94 grade	82	99.5	[26]
UVEX-FFP2	80	≥99	[27]
3M 1860	88.26	≥99	[28]
3M 1870+Aura^{TM}	69.73	≥99	[28]

A surface analysis was conducted for the samples, which were proceeded adsorption experiments before and after the adsorption of PVDF-HFP/PLA samples. As can be seen from the SEM image in Fig. 6b, the round particles adhered to the fiber surface were KCl particles collected on the fiber during the filtration experiment.

Table 1 summarizes the differential pressure, and filtration performance of commercially available masks used to compare the performance of the PVDF-HFP/PLA sample with that of air filters employed. In the case of commercial masks, the surface exposed to the exterior and inner surface in touch with the respiratory organ were made of spun bonded fiber with 1 or 2 sheets of melt-blown fibers sandwiched in between. As a result, it was proven that the differential pressure in the overlapped filter form of many layers was more than that of the filter created in this study to achieve excellent filtration performance. Adjusting the filter thickness and

increasing the spinning time of the simultaneously spun sample could result in improved filtering performance.

4. CONCLUSIONS

The global demand for personal masks has risen sharply due to the covid-19 pandemic and air pollution. In this regards, many studies on a better mask that lowers breathing resistance while maintaining filter performance has been steadily progressing. In this study, we successfully composite two different polar polymers into nanofibers via the co-spinning of solution blowing. In particular, PLA and PVDF-HFP fibers were chosen to be entangled together in a layer with a diameter of 1.05 μm and 0.33 μm, respectively. The mean pore diameter of each fiber is 12.57 μm and 3.1 μm, but that of composite filter was measured to 5.78 μm. The composite nanofilters made of two different polar materials showed filtration efficiency of up to 87% that is even higher than each PLA (59%) and PVDF-HFP (71%) while keep the differential pressure not to increases (32 Pa). From the aforementioned strategy, it is expected to improve the personal mask materials to reduce the breath resistance with high filtration performance.

ACKNOWLEDGEMENT

We are grateful for the financial support from the Korea Institute of Science and Technology (KIST) Institutional Program.

REFERENCES

1. Kodros, J.K., O'Dell, K., Samet, J.M., L'Orange, C., Pierce, J.R., and Volckens, J., "Quantifying the Health Benefits of Face Masks and Respirators to Mitigate Exposure to Severe Air Pollution," *GeoHealth*, Vol. 5, No. 9, 2021, p. e2021GH000482.
2. Chowdhury, M.A., Shuvho, M.B.A., Shahid, M.A., Haque, A.K.M.M., Kashem, M.A., Lam, S.S., Ong, H.C., Uddin, M.A., and Mofijur, M., "Prospect of Biobased Antiviral Face Mask to Limit the Coronavirus Outbreak," *Environmental Research*, Vol. 192, 2021, p. 110294.
3. Cheng, V.C.-C., Wong, S.-C., Chuang, V.W.-M., So, S.Y.-C., Chen, J.H.-K., Sridhar, S., To, K.K.-W., Chan, J.F.-W., Hung, I.F.-N., Ho, P.-L., and Yuen, K.-Y., "The Role of Community-wide Wearing of Face Mask for Control of Coronavirus Disease 2019 (COVID-19) Epidemic Due to SARS-CoV-2," *Journal of Infection*, Vol. 81, No. 1, 2020, pp. 107-114.
4. Fikenzer, S., Uhe, T., Lavall, D., Rudolph, U., Falz, R., Busse, M., Hepp, P., and Laufs, U., "Effects of Surgical and FFP2/N95 Face Masks on Cardiopulmonary Exercise Capacity," *Clinical Research in Cardiology*, Vol. 109, No. 12, 2020, pp. 1522-1530.
5. Wu, W., Sota, H., Hirogaki, T., and Aoyama, E., "Investigation of Air Filter Properties of Nanofiber Non-woven Fabric Manufactured by a Modified Melt-blowing Method Along with Flash Spinning Method," *Precision Engineering*, Vol. 68, 2021, pp. 187-196.
6. Bai, Y., Han, C.B., He, C., Gu, G.Q., Nie, J.H., Shao, J.J., Xiao, T.X., Deng, C.R., and Wang, Z.L., "Washable Multilayer Triboelectric Air Filter for Efficient Particulate Matter PM2.5 Removal," *Advanced Functional Materials*, Vol. 28, No. 15, 2018, p. 1706680.
7. Wang, Z., and Pan, Z., "Preparation of Hierarchical Structured Nano-sized/porous Poly(lactic acid) Composite Fibrous Membranes for Air Filtration," *Applied Surface Science*, Vol. 356, 2015, pp. 1168-1179.
8. Gao, H., Yang, Y., Akampumuza, O., Hou, J., Zhang, H., and Qin, X., "A Low Filtration Resistance Three-dimensional Composite Membrane Fabricated via Free Surface Electrospinning for Effective PM2.5 Capture," *Environmental Science: Nano*, Vol. 4, No. 4, 2017, pp. 864-875.
9. Yang, Y., Zhang, S., Zhao, X., Yu, J., and Ding, B., "Sandwich Structured Polyamide-6/polyacrylonitrile Nanonets/bead-on-string Composite Membrane for Effective Air Filtration," *Separation and Purification Technology*, Vol. 152, 2015, pp. 14-22.
10. Roh, S., Song, M., Lee, K., Park, K., and Kim, J., "Experimental and Computational Investigation of Intra- and Interlayer Space for Enhanced Depth Filtration and Reduced Pressure Drop," *ACS Applied Materials & Interfaces*, Vol. 12, No. 41, 2020, pp. 46804-46815.
11. Zhang, S., Liu, H., Yin, X., Yu, J., and Ding, B., "Anti-deformed Polyacrylonitrile/Polysulfone Composite Membrane with Binary Structures for Effective Air Filtration," *ACS Applied Materials & Interfaces*, Vol. 8, No. 12, 2016, pp. 8086-8095.
12. Gao, Y., Zhang, J., Su, Y., Wang, H., Wang, X.-X., Huang, L.-P., Yu, M., Ramakrishna, S., and Long, Y.-Z., "Recent Progress and Challenges in Solution Blow Spinning," *Materials Horizons*, Vol. 8, No. 2, 2021, pp. 426-446.
13. Sabbatier, G., Abadie, P., Dieval, F., Durand, B., and Laroche, G., "Evaluation of an Air Spinning Process to Produce Tailored Biosynthetic Nanofibre Scaffolds," *Materials Science and Engineering: C*, Vol. 35, 2014, pp. 347-353.
14. Bilbao-Sainz, C., Chiou, B.-S., Valenzuela-Medina, D., Du, W.-X., Gregorski, K.S., Williams, T.G., Wood, D.F., Glenn, G.M., and Orts, W.J., "Solution Blow Spun Poly(lactic acid)/hydroxypropyl Methylcellulose Nanofibers with Antimicrobial Properties," *European Polymer Journal*, Vol. 54, 2014, pp. 1-10.
15. Souza, M.A., Sakamoto, K.Y., and Mattoso, L.H.C., "Release of the Diclofenac Sodium by Nanofibers of Poly(3-hydroxybutyrate-co-3-hydroxyvalerate) Obtained from Electrospinning and Solution Blow Spinning," *Journal of Nanomaterials*, Vol. 2014, 2014, Article No. 56.
16. Akentjew, T.L., Terraza, C., Suazo, C., Maksimcuka, J., Wilkens, C.A., Vargas, F., Zavala, G., Ocaña, M., Enrione, J., García-Herrera, C.M., Valenzuela, L.M., Blaker, J.J., Khoury, M., and Acevedo, J.P., "Rapid Fabrication of Reinforced and Cell-laden Vascular Grafts Structurally Inspired by Human Coronary Arteries," *Nature Communications*, Vol. 10, No. 1, 2019, p. 3098.
17. Deng, N., Kang, W., Ju, J., Fan, L., Zhuang, X., Ma, X., He, H., Zhao, Y., and Cheng, B., "Polyvinyl Alcohol-derived Carbon

Nanofibers/carbon Nanotubes/sulfur Electrode with Honeycomb-like Hierarchical Porous Structure for the Stable-capacity Lithium/sulfur Batteries," *Journal of Power Sources*, Vol. 346, 2017, pp. 1-12.
18. Jia, K., Zhuang, X., Cheng, B., Shi, S., Shi, Z., and Zhang, B., "Solution Blown Aligned Carbon Nanofiber Yarn as Supercapacitor Electrode," *Journal of Materials Science: Materials in Electronics*, Vol. 24, No. 12, 2013, pp. 4769-4773.
19. Xu, X., Li, R., Tang, C., Wang, H., Zhuang, X., Liu, Y., Kang, W., and Shi, L., "Cellulose Nanofiber-embedded Sulfonated Poly (ether sulfone) Membranes for Proton Exchange Membrane Fuel Cells," *Carbohydrate Polymers*, Vol. 184, 2018, pp. 299-306.
20. Wang, H., Zhuang, X., Wang, X., Li, C., Li, Z., Kang, W., Yin, Y., Guiver, M.D., and Cheng, B., "Proton-Conducting Poly-γ-glutamic Acid Nanofiber Embedded Sulfonated Poly(ether sulfone) for Proton Exchange Membranes," *ACS Applied Materials & Interfaces*, Vol. 11, No. 24, 2019, pp. 21865-21873.
21. Choi, S., Lee, H.M., and Kim, H.S., "High Performance And Moisture Stable Humidity Sensors Based on Polyvinylidene Fluoride Nanofibers by Improving Electric Conductivity," *Polymer Engineering & Science*, Vol. 59, No. 2, 2019, pp. 304-310.
22. Khattab, T.A., Rehan, M., Aly, S.A., Hamouda, T., Haggag, K.M., and Klapötke, T.M., "Fabrication of PAN-TCF-hydrazone Nanofibers by Solution Blowing Spinning Technique: Naked-eye Colorimetric Sensor," *Journal of Environmental Chemical Engineering*, Vol. 5, No. 3, 2017, pp. 2515-2523.
23. Shi, L., Zhuang, X., Tao, X., Cheng, B., and Kang, W., "Solution Blowing Nylon 6 Nanofiber Mats for Air Filtration," *Fibers and Polymers*, Vol. 14, No. 9, 2013, pp. 1485-1490.
24. Khalid, B., Bai, X., Wei, H., Huang, Y., Wu, H., and Cui, Y., "Direct Blow-Spinning of Nanofibers on a Window Screen for Highly Efficient PM2.5 Removal," *Nano Letters*, Vol. 17, No. 2, 2017, pp. 1140-1148.
25. Jia, C., Liu, Y., Li, L., Song, J., Wang, H., Liu, Z., Li, Z., Li, B., Fang, M., and Wu, H., "A Foldable All-Ceramic Air Filter Paper with High Efficiency and High-Temperature Resistance," *Nano Letters*, Vol. 20, No. 7, 2020, pp. 4993-5000.
26. Jung, S., Hemmatian, T., Song, E., Lee, K., Seo, D., Yi, J., and Kim, J., "Disinfection Treatments of Disposable Respirators Influencing the Bactericidal/Bacteria Removal Efficiency, Filtration Performance, and Structural Integrity," *Polymers*, Vol. 13, No. 1, 2021, pp. 45.
27. He, W., Guo, Y., Gao, H., Liu, J., Yue, Y., and Wang, J., "Evaluation of Regeneration Processes for Filtering Facepiece Respirators in Terms of the Bacteria Inactivation Efficiency and Influences on Filtration Performance," *ACS Nano*, Vol. 14, No. 10, 2020, pp. 13161-13171.
28. Grillet, A.M., Nemer, M.B., Storch, S., Sanchez, A.L., Piekos, E.S., Leonard, J., Hurwitz, I., and Perkins, D.J., "COVID-19 Global Pandemic Planning: Performance and Electret Charge of N95 Respirators after Recommended Decontamination Methods," *Experimental Biology and Medicine*, Vol. 246, No. 6, 2020, pp. 740-748.